

Stability and heat transfer of rotating cryogenes.

Part 2. Effects of rotation on heat-transfer properties of convection in liquid ^4He

By J. M. PFOTENHAUER, P. G. J. LUCAS†
AND R. J. DONNELLY

Department of Physics, University of Oregon, Eugene, OR 97403

(Received 13 October 1983 and in revised form 23 March 1984)

Heat-transfer measurements have been made in normal liquid ^4He contained within a rotating, cylindrical, cryogenic Bénard cell with variable aspect ratio. Data are presented for a range of dimensionless angular velocities $0 \leq \Omega < 600$ and Prandtl numbers $0.49 \leq Pr \leq 0.76$ and for three aspect ratios Γ of 7.81, 4.93 and 3.22. Where possible, comparisons are made with theoretical predictions and past experiments concerning heat transfer in rotating fluids.

1. Introduction

The heat-transfer properties of a rotating Bénard convection system have received sparse attention in the experimental arena compared to that given them by the many theoretical papers of the past few decades. There are early experimental reports by Fultz & Nakagawa (1955) and by Dropkin & Globe (1959) concerning the effect of rotation on the heat transport through convecting mercury. A later study by Koschmieder (1967) reports on a rotating Bénard system in which silicone oil is used as the convecting fluid. Koschmieder's results imply increases in heat transfer at Rayleigh numbers below those critical values given by linear stability theory, and he demonstrates that these effects are most likely caused by centrifugally induced flows. A significant amount of heat-transfer data is presented by Rossby (1969), using water and mercury. The results he obtained with mercury verified some aspects of Veronis' (1968) finite-amplitude effect predictions, but those obtained with water presented some unexpected results which will be discussed later in this paper. These few reports comprise the experimental work on heat transfer in a rotating Bénard system. The theoretical work, on the other hand, is rich in both quantity and variety of topics addressed. A few examples are the papers by Veronis (1959, 1966, 1968) introducing finite-amplitude effects, those by Daniels & Stewartson (1977, 1978*a*) on spatial oscillations and overstability, those by Homsy & Hudson (1971, 1972) on cell-size and centrifugal effects, and that by Clever & Busse (1979) on stability boundaries.

Apart from their own intrinsic interest, past work has shown that heat-transfer properties can be helpful in understanding other related properties of thermal convection. In the non-rotating case there are a number of examples. For some time discrepancies existed between theory and experiment regarding the dependence of the wavelength of the convection pattern and the magnitude of the heat transfer on the supercritical Rayleigh number. Willis, Deardorff & Sommerville (1972) resolved

† Permanent address: Department of Physics, The University, Manchester M13 9 PL, England.

both discrepancies by showing that compatible Nusselt numbers could be obtained if one used larger wavelengths (as seen in experiment) in the analysis predicting the heat transfer. The recent heat-transfer work of Behringer & Ahlers (1982) demonstrates the development of stable and metastable patterns of convection, each displaying different heat-transfer characteristics. A related report by Ahlers *et al.* (1981) gives additional information regarding these stable and metastable states, suggesting that they may be concentric rolls and hexagons respectively.

The experimental heat-transfer report presented here is given in part as a response to the many theoretical predictions, and in part as an aid to understanding the general properties of a convecting fluid under the influence of rotation. In §2 we give a brief description of the apparatus used and the method of data gathering, as well as comments regarding the uncertainties involved in the data. Section 3 contains a discussion of the initial slopes of the nonlinear heat-transfer data and includes a description of nonlinear heat transfer for the subcritical mode of convection referred to in Part 1 (Lucas, Pfotenhauer & Donnelly 1983). This is done in order to gather all the heat-transfer data in the present paper. A detailed experimental investigation of the subcritical mode is presently in progress. Section 4 contains a discussion of heat-transfer enhancement by rotation. A summary discussion is given in §5.

2. Apparatus and data acquisition

We have conducted experiments using helium I, the normal phase of liquid helium (above the lambda transition) to study the heat transfer of a rotating convection system in cylindrical cells of aspect ratios $\Gamma = 7.81, 4.93, 3.22$ (where Γ is defined as the ratio of the cell's radius R to its height d). The dimensions and the related uncertainties of these cells are given in table 1. Here the wall thickness is represented by δ . The bulk of the data presented in this paper is from work done with the $\Gamma = 7.81$ cell, the design of which has been presented in Part 1. The design of the $\Gamma = 4.93$ and 3.22 cells is shown in figure 1. All electrical connections are the same as for the $\Gamma = 7.81$ cell, and these details are omitted for clarity. Note that the stainless-steel wall is made to be an interchangeable part, sealed to the copper pieces with indium O-rings and bolts, thus giving freedom and relative ease in changing Γ by changing the cell height d . A helium reservoir has been added to the basic cell design described in Part 1 to facilitate the use of a free surface for the liquid to maintain its pressure at the saturated vapour pressure. Helium is condensed into the reservoir from a fill line connected to a volume of ^4He gas as described in Part 1. A 0.16 cm hole has been drilled into the bottom of the reservoir, to about halfway down through the top of the upper copper boundary of the cell, at which point the hole turns, coming out of the copper to the inside of the stainless-steel cylinder, which defines the vertical wall. Even with the press fit of the copper boundary in the stainless-steel cylinder, there is sufficient room for helium to flow from the reservoir to the cell; thus the cell is filled in the same condensing process that partially fills the reservoir.

We were careful both in the machining and assembly of the $\Gamma = 4.93$ and 3.22 cells to ensure that the two copper pieces defining the horizontal cell boundaries were parallel. It is expected (Behringer & Ahlers 1982) that if they were not parallel some rounding of the Nusselt-number Nu , Rayleigh-number Ra data would show up near R_c , the critical value of the Rayleigh number above which the fluid convects. Should rounding of this sort appear, it would do so in every run and would not disappear unless the boundaries were made parallel. The majority of our runs, both rotating and non-rotating, displayed essentially no rounding. α , as defined below, is typically

Γ	R (cm)	d (cm)	δ (cm)
7.81	1.245 (0.001)	0.1595 (0.0007)	0.025 (0.0013)
4.93	0.809 (0.001)	0.164 (0.001)	0.017 (0.0013)
3.22	0.809 (0.001)	0.251 (0.001)	0.017 (0.0013)

TABLE 1. Cell dimensions and their uncertainties

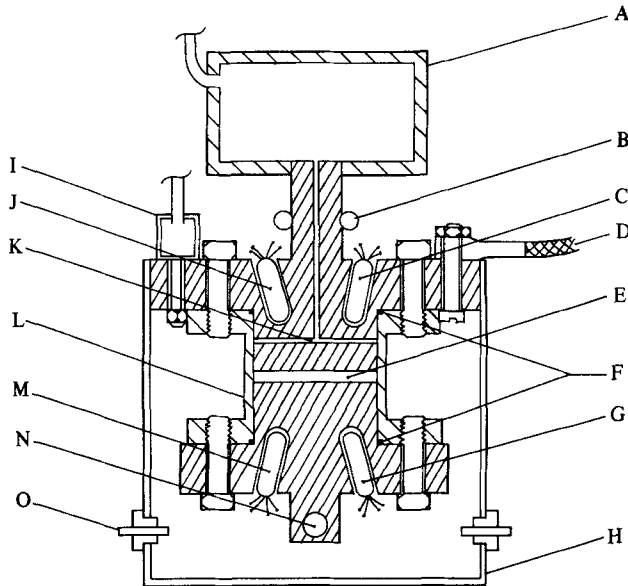


FIGURE 1. Rayleigh-Bénard experimental cell: A, stainless-steel walls of helium reservoir; B, toroidal metal film resistor H_c ; C, germanium resistance thermometer R_{DC} ; D, copper-braid heat leak to bath; E, volume occupied by fluid; F, 0.05 cm indium O-ring; G, germanium resistance thermometer R_{DF} ; H, copper thermal shield clamped to upper boundary; I, vapour-pressure bulb; J, germanium resistance thermometer R_c ; K, fill line from reservoir to cell; L, interchangeable stainless-steel tube defining vertical cell walls; M, germanium resistance thermometer R_F ; N, metal-film resistor H_F ; O, feedthrough.

of order 0.001. In a few cases, however, experimental noise produced data that appeared to be rounded. We define the amount of rounding in the following manner. The critical Rayleigh number R_c is determined by a quadratic fit to the Nusselt-number, Rayleigh-number data as described in §5.2 of Part 1. We can then define the parameter $\epsilon = Ra/R_c$. For a rounded transition there would be some $\epsilon' < 1$ for which $Nu(\epsilon')$ rises above unity by some threshold amount. A reasonable experimental value for this threshold is $Nu = 1.005$. The amount of rounding can then be quantified by the parameter $\alpha = 1 - \epsilon'$. For the non-rotating runs the largest value of α was 0.09, while α was of order 0.001 for the rotating runs. Since the apparent rounding appeared in only a very few of all the runs, we have concluded that the horizontal boundaries are parallel to each other and the Earth's surface and perpendicular to the axis of rotation.

All raw data (that is, W_F , the heat input at the bottom of the cell, and ΔT , the resultant temperature difference across the cell) have been recorded and reduced to Rayleigh-number, Nusselt-number form as described in Part 1. The angular rotation

rate Ω_D is converted to dimensionless form by putting $\Omega = \Omega_D d^2/\nu$, where ν is the kinematic viscosity. For comparison, the Taylor number is defined as $Ta = 4\Omega^2$. In the data that are presented below, least-squares fits are made to the (Nu, Ra) -data, and uncertainties are given for the coefficients obtained from these fits. In recent data that we have taken (for which $\Gamma = 3.22$), we observed fluctuations in successive measurements of ΔT . These uncertainties were typically about $7 \mu\text{K}$ and should be compared with critical values of ΔT from $\sim 0.5 \text{ mK}$ for $\Omega = 0$ to $\sim 50 \text{ mK}$ for the high-rotation runs. The uncertainties in ΔT , together with the uncertainties in W_F (typically 0.5% of W_F) given by the resolution of our voltmeter and ammeter, enabled us to calculate the uncertainties in Nu . These were necessary to obtain the uncertainties for the coefficients of the fits we discuss below. For data taken before this statistical analysis of ΔT was implemented, the uncertainties in Nu for a given run were taken to be all equal and approximated by the square root of the sample variance. That is,

$$\sigma_{Nu} = \left[\frac{1}{N-n} \sum_i [Nu_i - f(Nu_i)]^2 \right]^{\frac{1}{2}}, \quad (1)$$

where N is the number of data points, $n-1$ is the degree of the polynomial fit, and $f(Nu_i)$ is the value of the polynomial function of Nu (at the point Nu_i) being fitted to the data. Both methods used to determine the uncertainties in the coefficients of the fits yielded very similar results for similar conditions.

3. Initial slopes of the nonlinear heat-transfer data

3.1. Data and fits

Each run of our experiment gathered Nusselt-number, Rayleigh-number data at a set rotation rate Ω , the range of rotation rates covered being $0 \leq \Omega < 600$. We also made rotation studies at various temperatures in the range $2.186 \text{ K} \leq T_C < 3.7 \text{ K}$, where T_C is the controlled temperature at the top of the cell. When no subcritical convection mode was observed (see §3.2) the values of the critical Rayleigh number R_c were determined as described in §5.2 of Part 1. We wish to note here a correction to the data presented in Part 1 for which $T_C = 3.178 \text{ K}$. Owing to a computer-programming error, an erroneous calibration was used to determine the values of ΔT at this value of T_C . The raw data have been reanalysed with the correct S versus ΔT calibration, and the resultant critical Rayleigh numbers appear in table 2. These corrected values fall very close to those obtained at $T_C = 2.63 \text{ K}$ and 2.4 K and leave all our critical Rayleigh numbers measured with helium I below the theoretical $R_c(\Omega)$ values.

We noted in Part 1 that the values of R_c for any given Ω were temperature-dependent and lower than the theoretical values of $R_c(\Omega)$, and we have attributed this discrepancy to imperfect values of the fluid parameters of helium I. The reader should note that, although the variation in R_c as a function of T_C (described in Part 1) is as large as 20% , determination of R_c at individual temperatures and rotation rates displayed a scatter of only a few per cent at most. This scatter is determined by the uncertainties in ΔT described in §2.

A few non-rotating runs performed with the $\Gamma = 4.93$ cell display R_c values (see table 2) close to those given in Part 1, and generally follow the temperature variations of R_c described in Part 1. For each run the data above R_c were fitted to the equation

$$Nu - 1 = \sum_i N_i \left(\frac{Ra}{R_c} - 1 \right)^i \quad (i = 1, 2, 3) \quad (2)$$

T_C	Pr	Γ	Ω	R_{sc}	R_c	
2.186	0.76	7.81	452	47 600	56 000	
			4.93	0	—	1 220
2.198	0.71	4.93	0	—	1 380	
2.24	0.61	4.93	0	—	1 280	
2.63	0.49	7.81	160	15 300	15 900	
			192	19 000	20 000	
			256	26 300	28 800	
			320	34 500	38 900	
			452	49 800	58 300	
			554	64 300	76 800	
			4.93	0	—	1 350
			121	10 600	11 000	
			145	12 900	13 500	
			193	17 700	19 100	
			217	20 200	21 900	
			241	23 300	25 200	
			3.22	100	8 010	18 430
			110	8 910	9 900	
135	10 800	12 400				
170	14 300	16 000				
194	16 400	18 900				
221	18 900	23 300				
3.1	0.53	4.93	0	—	1 370	
3.178	0.55	7.81	0	—	1 370†	
			32	—	2 830†	
			64	—	5 400†	
			96	—	8 330†	
			128	—	11 500†	
			160	—	15 200†	
			192	—	19 200†	
			452	49 800	57 000	
			554	63 200	74 000	

† Values revised from those appearing in table 2 of Part 1.

TABLE 2. Values of subcritical and critical Rayleigh numbers

by a method of least squares in order to determine the coefficients N_i as well as the uncertainties in those coefficients. We have investigated the effects of varying R_c over the range corresponding to the uncertainty in ΔT on the deduced values of N_1 and N_2 . This variation of R_c modifies the values of N_1 and N_2 by less than 2% in the worst case. The upper bound of the Rayleigh number used in the fits was chosen to be $Ra \approx 1.5R_c$. This enabled the convexity of the Nusselt number as a function of the reduced Rayleigh number, as well as the initial slope N_1 , to be determined. The standard χ^2 goodness-of-fit test (see e.g. Bevington 1969) was used to determine whether a cubic, quadratic or linear form of (2) produced the best fit to the data. In all but a few cases the quadratic form afforded the best fit. Results for N_1 , σ_{N_1} , N_2 and σ_{N_2} as well as T_C , Γ , Ω and the Prandtl number $Pr = \nu/D_T$ (D_T is the thermal diffusivity of the fluid) at temperature T_C for the various runs are presented in table 3.

Because of the variation in values of R_c with T_C , we have concentrated on one temperature, $T_C = 2.63$ K, for which $Pr = 0.49$. The majority of graphs and discussion

T_C	Pr	Γ	Ω	$N_1(\sigma_{N_1})$	$N_2(\sigma_{N_2})$			
2.186	0.76	7.81	0	0.940 (0.033)	-0.488 (0.063)			
			16	0.934 (0.054)	-0.268 (0.101)			
			32	1.108 (0.057)	-0.382 (0.104)			
			64	1.188 (0.042)	-0.330 (0.079)			
			452	2.058 (0.068)	0.022 (0.128)			
		4.93	0	0.597 (0.187)	0.226 (0.457)			
2.198	0.71	4.93	0	0.779 (0.036)	-0.172 (0.102)			
2.24	0.61	4.93	0	0.822 (0.060)	-0.351 (0.112)			
2.4	0.51	7.81	0	0.989 (0.053)	-0.559 (0.106)			
			32	1.053 (0.087)	-0.027 (0.179)			
			64	1.256 (0.055)	-0.365 (0.105)			
			96	1.334 (0.050)	-0.403 (0.098)			
			128	1.450 (0.034)	-0.428 (0.060)			
			160	1.591 (0.046)	-0.410 (0.077)			
			192	1.635 (0.082)	-0.373 (0.162)			
					7.81	0	0.758 (0.048)	-0.245 (0.089)
2.63	0.49	7.81	32	1.164 (0.049)	-0.406 (0.086)			
			64	1.104 (0.018)	-0.170 (0.032)			
			96	1.379 (0.062)	-0.488 (0.105)			
			128	1.482 (0.027)	-0.428 (0.042)			
			160	1.467 (0.023)	-0.282 (0.049)			
			192	1.572 (0.022)	-0.280 (0.047)			
			256	1.715 (0.037)	-0.120 (0.090)			
			320	1.806 (0.064)	-0.022 (0.187)			
			452	2.058 (0.018)	-0.122 (0.037)			
			554	2.226 (0.036)	-0.252 (0.080)			
					4.93	0	0.660 (0.043)	-0.130 (0.070)
						121	1.603 (0.026)	-0.706 (0.055)
						145	1.655 (0.031)	-0.616 (0.067)
						193	1.694 (0.033)	-0.433 (0.072)
			217	1.688 (0.035)	-0.323 (0.086)			
			241	1.724 (0.039)	-0.266 (0.079)			
		3.22	100	1.407 (0.080)	-0.395 (0.212)			
			110	1.528 (0.016)	-0.546 (0.021)			
			135	1.779 (0.027)	-0.990 (0.059)			
			170	1.636 (0.025)	-0.481 (0.047)			
			193	1.800 (0.020)	-0.703 (0.037)			
			220	1.812 (0.039)	-0.597 (0.071)			
3.1	0.53	4.93	0	0.619 (0.090)	-0.226 (0.100)			
3.178	0.55	7.8	0	0.922 (0.095)				
			32	0.848 (0.026)				
			64	1.183 (0.095)	-0.397 (0.192)			
			96	1.318 (0.039)	-0.426 (0.086)			
			128	1.278 (0.051)	-0.221 (0.100)			
3.178	0.55	7.81	160	1.495 (0.017)	-0.339 (0.029)			
			192	1.509 (0.034)	-0.199 (0.073)			
			452	1.974 (0.013)	0.204 (0.030)			
			554	2.075 (0.013)	0.378 (0.027)			
					7.81	0	0.679 (0.108)	0.021 (0.212)
3.425	0.59	7.81	32	1.029 (0.215)	-0.115 (0.386)			
			64	1.175 (0.064)	-0.320 (0.107)			
			96	1.280 (0.075)	-0.336 (0.131)			
			128	1.408 (0.081)	-0.319 (0.153)			
					7.81	0	0.679 (0.108)	0.021 (0.212)

T_C	Pr	Γ	Ω	$N_1(\sigma_{N_1})$	$N_2(\sigma_{N_2})$
3.635	0.63	7.81	160	1.392 (0.029)	-0.144 (0.064)
			192	1.557 (0.042)	-0.247 (0.067)
			32	1.095 (0.095)	-0.115 (0.172)
			64	1.142 (0.086)	-0.154 (0.142)
			96	1.323 (0.076)	-0.291 (0.144)
			128	1.651 (0.027)	-0.590 (0.050)
			160	1.627 (0.054)	-0.405 (0.101)
			192	1.580 (0.027)	-0.165 (0.053)

TABLE 3. Summary of heat-transfer coefficients for various Pr , Γ and Ω

that follow thus apply most directly to that case (the obvious exception being §4.2). The general trends mentioned are, however, true of data gathered at the other temperatures.

In figure 2 we have displayed N_1 , the initial slope, as a function of Ω for runs at $T_C = 2.63$ and $\Gamma = 7.81$, with figure 3 showing some of the data in the $(Nu, Ra/R_C)$ -form from which the initial slopes were computed. From the data shown in figures 2 and 3, and from the data for all Pr given in table 3, it can be seen that N_1 displays a large increase as Ω is increased to approximately 100. As Ω is further increased, N_1 continues to increase, although at a slower rate. From the calculations and results given by Veronis (1968) for $Pr = 6.8$, $\Gamma = \infty$ and for $0 \leq \Omega < 160$ (see especially table 1 and figure 2 of his paper), it is clear that one should expect an increase in N_1 as Ω is increased from 0. The results given by Veronis imply an initial slope rising from 1.2 for $\Omega = 0$ to 1.6 for $\Omega = 158$. Though our data for $Pr = 0.51$ and $\Gamma = 7.81$ give initial slopes slightly smaller than those obtainable from Veronis' results, the general behaviour is the same.

The use of the initial slope as a measure of the increase of heat transfer above the onset of convection has received repeated attention in the literature pertaining to non-rotating systems, and as Behringer & Ahlers (1982) report, there is good agreement between experiment and theory regarding the dependence of the initial slope on the aspect ratio Γ ; that is, for $\Omega = 0$ the initial slope increases with Γ . Charlson & Sani (1975) have attributed this behaviour to an increasing stabilizing effect of the sidewalls on the convective motions as Γ is decreased. Ahlers *et al.* (1982) also argue that more than one convective pattern is likely to exist near R_C and these different patterns produce different values of N_1 . Our data for $\Gamma = 7.81$ and $\Omega = 0$ fall roughly in two groups, one centred around $N_1 = 0.7$ and the other centred around $N_1 = 0.96$. For comparison, Behringer & Ahlers (1982) obtain $N_1 = 0.83$ for their cell A of aspect ratio $\Gamma = 4.72$ in its stable mode. There is obvious scatter in our data from one Prandtl number to another. We believe these variations are real and that they reflect variations in heat transfer from different convective patterns, or a mixture thereof, present in our data.

We have also observed that N_1 increases with Γ when $\Omega = 0$. Data taken at $T_C = 2.186$ K and at $T_C = 2.63$ K (see table 3) have confirmed this behaviour. However, as the data taken at $T_C = 2.63$ K for higher values of Ω display (see figure 4), this dependence is reversed in the range $100 < \Omega < 250$. The reason for this reversal is possibly connected with the subcritical convective mode (discussed in §3.2), but it is clear that sidewalls do not have as stabilizing an effect on the heat transfer of a rotating convection system as they do in the non-rotating case.

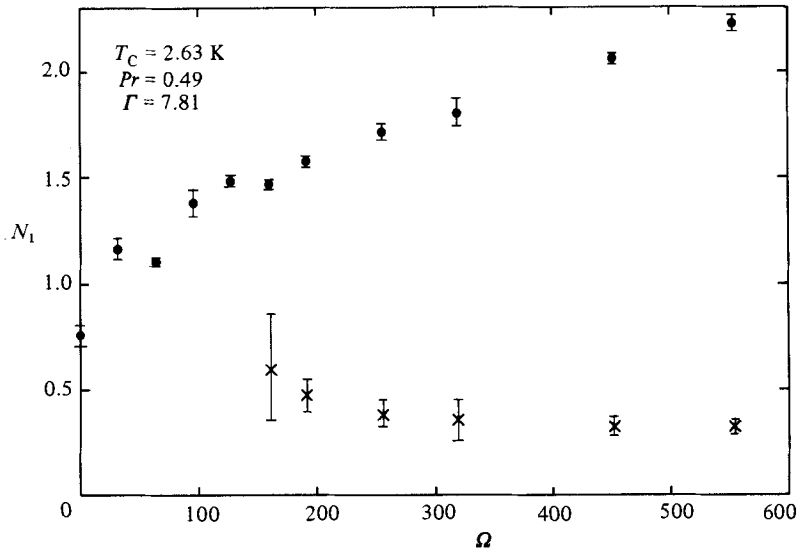


FIGURE 2. The effect of rotation on the initial slope N_1 of heat transfer: \bullet , N_1 for convection above R_c ; \times , N_1 for convection in subcritical mode.

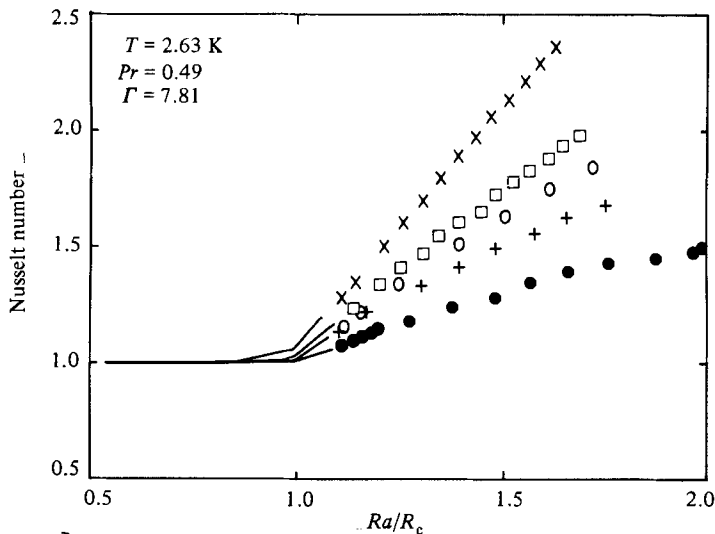


FIGURE 3. Nusselt number *vs.* reduced Rayleigh number; a composite plot of $(Nu, Ra/R_c)$ -data for various rotation rates: \bullet , $\Omega = 0$; +, 32; \circ , 128; \square , 192; \times , 452. Data for $Ra/R_c < 1.1$ are given as solid lines for clarity. The data from runs for which $\Omega = 32$ and 128 are essentially the same below $Ra/R_c = 1.1$ and are represented by a single line.

3.2. Subcritical heat transfer

In table 4 we present some initial heat-transport data on a convective mode which we have referred to as 'subcritical' in Part 1. The term subcritical is used in the following sense. In runs at individual temperatures, and at all values of Ω for which no subcritical convection is observed, values of R_c fall at a certain percentage below the theoretical values of $R_c(\Omega)$. This discrepancy is attributed to faulty knowledge of the fluid parameters of helium I. The observed values of $R_c(\Omega)$ at $T_c = 2.63$ K, for instance, all fall $\sim 10\%$ below the theoretical values. When the subcritical mode

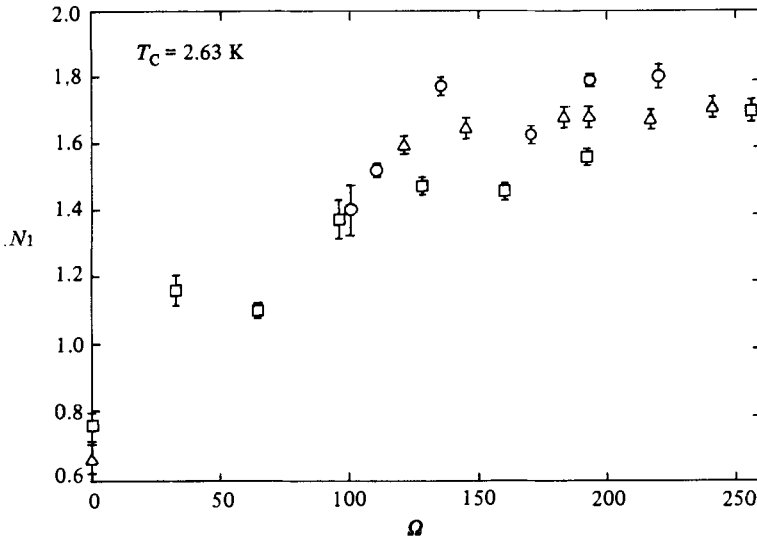


FIGURE 4. Influence of aspect ratio on initial slopes; N_1 is shown as a function of Ω with Γ as a parameter: \square , $\Gamma = 7.81$; \triangle , 4.93; \circ , 3.22.

T_C	Pr	Γ	Ω	$N_1(\sigma_{N_1})$	$N_2(\sigma_{N_2})$
2.186	0.76	7.81	452	0.457 (0.075)	-0.687 (0.659)
3.178	0.55	7.81	452	0.510 (0.072)	-1.08 (0.488)
			554	0.357 (0.074)	-0.080 (0.416)
2.63	0.49	7.81	160	0.607 (0.252)	
			192	0.470 (0.075)	
			256	0.386 (0.062)	
			320	0.349 (0.093)	
			452	0.323 (0.045)	0.022 (0.234)
			554	0.323 (0.028)	
		4.93	121	0.387 (0.273)	
			145	0.721 (0.207)	
			193	0.595 (0.132)	
			217	0.529 (0.125)	
			241	0.519 (0.079)	
		3.22	100	1.544 (0.675)	-18.7 (14.3)
			110	1.442 (0.085)	-6.05 (0.69)
			135	0.622 (0.026)	
			170	0.574 (0.025)	
193	0.771 (0.015)				
220	0.693 (0.023)				
1000	0.864 (0.001)				
1347	0.925 (0.001)				

TABLE 4. Subcritical heat-transfer coefficients

is present with its initial increase in Nu , another change in the heat-transfer slope occurs at higher Rayleigh numbers. These higher values of Ra are the same percentage ($\sim 10\%$ for $T_C = 2.63$ K) below the theoretical values of $R_c(\Omega)$, leading one to associate this critical Rayleigh number with the onset of steady convection as predicted by the standard theories. The first increase in Nu is thus at R_{sc} , some

subcritical value of the Rayleigh number. It is worth noting here that Homsy & Hudson (1971) have reanalysed data taken by Rossby (1969) displaying subcritical flows in water, and show that in Rossby's data the second and larger increase in Nu occurred at Rayleigh numbers coincident with the theoretical values of $R_c(\Omega)$.

The values of R_{sc} were determined in the same way as R_c was determined when the subcritical mode was not present. When the subcritical mode was present, the experimental values of R_c were determined by the intersection of the fit to the subcritical data with the quadratic fit to the data above the second increase in Nusselt number. Table 2 lists values of R_c , obtained since publication of Part 1, as well as values of R_{sc} .

Considering the increase in N_1 with decreasing Γ mentioned in §3.1, we have noted (as did Rossby) that a decrease in Γ results in larger increase in Nu above R_{sc} . It is likely that above R_c the normal convective flow would be superimposed on the subcritical flow and thus the effects of a decrease in Γ , for a fixed Ω , would show up as an increased N_1 even in the normal convective flow.

4. Inhibitions and enhancements of heat transfer

4.1. General inhibitions

From table 3 and figures 2, 3 and 4, one might get the impression that convective heat transfer is generally enhanced by rotation. In fact the opposite is true; rotation has an inhibiting effect on convective motions. We have shown in Part 1 that the onset of convection is inhibited by rotation, as was predicted by Chandrasekhar (1961) and others. Rotation also inhibits the amplitude of convection or the heat transfer, once convection sets in. This is demonstrated in figure 5, where it can be seen that, once the fluid is convecting, $d(Nu)/d(Ra)$ decreases with increasing Ω . Veronis (1966) attributed this inhibiting effect of rotation on the amplitude of convection to a 'geophysical thermal wind'. The explanation given is basically that the Coriolis force produces a vertical shear perpendicular to the horizontal flow in a convecting cell, and this shear then inhibits the amplitude of that flow. The term 'thermal wind' is given because the horizontal flows are driven by (and proportional to) the horizontal temperature gradient of the perturbed temperature field.

One should not see the decrease of $d(Nu)/d(Ra)$ as contradicting the increase of N_1 with Ω , indeed the two behaviours are simply related since $N_1 = R_c[d(Nu)/d(Ra)]$. Thus N_1 increases with Ω , since the increase in R_c with Ω is greater than the decrease in $d(Nu)/d(Ra)$ with Ω .

4.2. An enhancement of heat transfer at small rotation rates

For small values of Ω and for a limited range of Pr , we found that $d(Nu)/d(Ra)$ increased with Ω – an exception to the observations presented in §4.1. A similar behaviour has in fact been predicted by Clever & Busse (1979). In figure 7 of their paper they show that for $Pr \ll 1$ and for $Ra - R_c = 2 \times 10^3$ one can expect a monotonic increase in Nu with Ω for $0 \leq \Omega \leq 50$. For $Pr > 1$, however, one can expect a monotonic decrease in Nu with increasing Ω . In the range $0.3 \leq Pr \leq 0.6$ there is a complicated region in which one should expect an increase in Nu from $\Omega = 0$ to $\Omega = 30$, but, as Ω is increased to 50, Nu drops again. Measuring Nu at this fixed distance above $R_c(\Omega)$ essentially measures the slope of the heat transfer above $R_c(\Omega)$.

In figure 6 we display data for $0 < \Omega < 100$, $0.49 < Pr < 0.76$, and for which $Ra - R_c = 2 \times 10^3$ (the dashed lines have no theoretical significance). The general behaviour suggested by Clever & Busse is verified; that is, in the region $Pr \approx 0.5$,

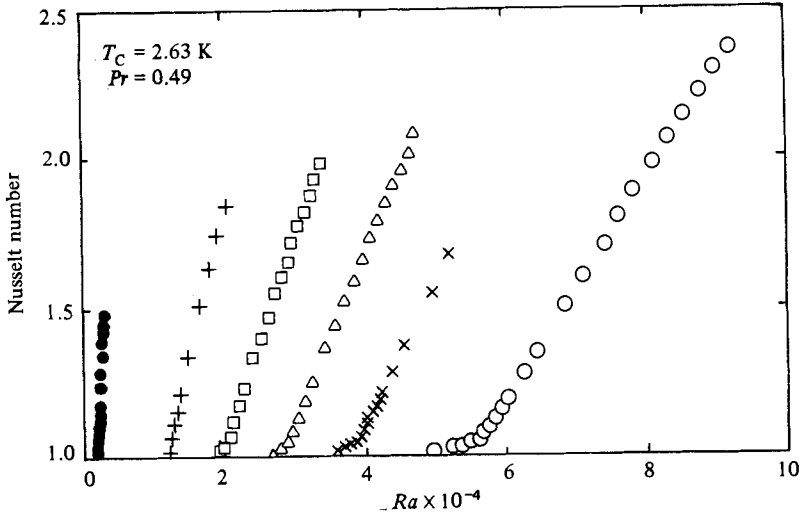


FIGURE 5. Inhibition of heat transfer; (Nu, Ra) -plots at various rotation rates displaying reduced heat transfer in convection with increasing Ω ; ●, $\Omega = 0$; +, 128; □, 192; △, 256; ×, 320; ○, 452.

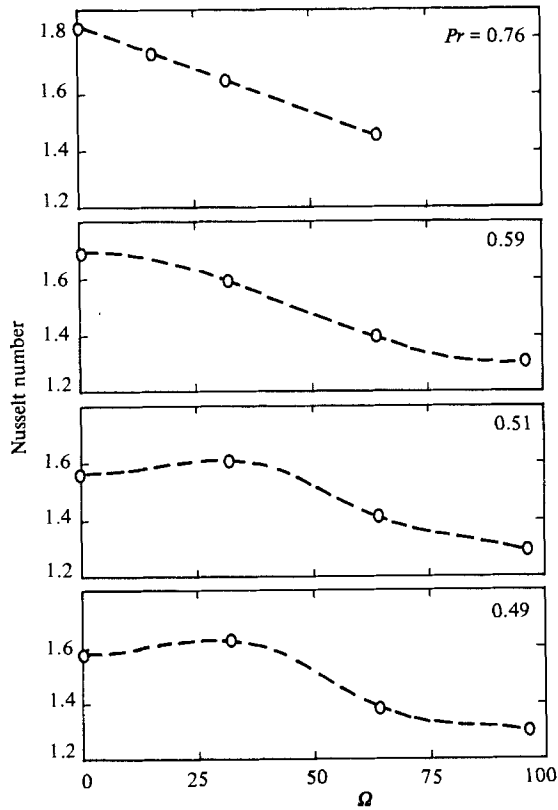


FIGURE 6. Relative enhancement of heat transfer; Nusselt numbers at $Ra - R_c = 2 \times 10^3$ as functions of rotation rate Ω and Prandtl number Pr . The dashed lines are simply a suggestion for the trend of the data.

Nu increases as Ω is increased from 0 to 30, and decreases for higher Ω , but, as Pr is increased to 0.76, the Nusselt number drops continuously as Ω is increased. This seemingly critical nature of $\Omega \approx 30$ should not be interpreted as resulting from the instability described by Küppers & Lortz (1969) and Küppers (1970), which occurs at $\Omega \approx 27$ for the Prandtl range of helium. Clever & Busse (1979) have suggested that the Nusselt number would not be sensitive to this instability. More importantly, however, whereas the analysis of Küppers & Lortz was for $Pr = \infty$ and extended by Küppers for all Pr , the results described here are expected *only* for the limited Prandtl-number range $0.3 < Pr < 0.6$.

The results of this investigation differ from the predictions of Clever & Busse, however, in one important aspect. Whereas Clever & Busse predict the changes in Nu with Pr to occur when $\Omega > 0$, we find the changes only for $\Omega = 0$. In particular, figure 6 shows that Nu at $Ra - R_c(\Omega) = 2 \times 10^3$ and for a given $\Omega > 0$ is essentially the same for all Pr . However, when $\Omega = 0$ the values of Nu increase as Pr increases from 0.49 to 0.76. Additional data taken in this manner for $\Omega = 0$ at $Pr = 0.61$ ($Nu = 1.68$) and $Pr = 0.71$ ($Nu = 1.79$) confirm this behaviour.

4.3. Investigation of heat-transfer enhancement at absolute Rayleigh number

In §§4.1 and 4.2 we have presented the dependence of Nu on Ra and Ω , but have done so always in terms of reduced Rayleigh numbers Ra/R_c or in terms of relative Rayleigh numbers $Ra - R_c$. We now discuss the effect of rotation on heat transfer in terms of absolute Rayleigh numbers. This approach affords us the opportunity of investigating an interesting phenomenon.

In his paper on a rotating cylindrical convection system, Rossby (1969) reported two unexpected results for heat transfer in water. One of these, the 'subcritical' convection, we have already mentioned and have confirmed in our experiments with helium I. The second unexpected result reported by Rossby shows a maximum Nusselt number for a fixed absolute Rayleigh number at some Taylor number other than 0; that is, for a given temperature difference, water transports more heat in convection while at a certain rotation rate than when not rotating. In their three-dimensional numerical analysis Sommerville & Lipps (1972) verified that one could expect the Nusselt number to have a maximum for a given Ra at some $\Omega > 0$ when $Pr = 6.8$. Rossby did not see this behaviour of heat transfer in mercury, which has a Prandtl number $Pr = 0.025$, about two orders of magnitude smaller. Our experiments with helium I afforded us the range of Prandtl number one order of magnitude smaller than that of water.

We have investigated similar ranges of (Ra, Nu, Ω) -space where Rossby's data showed a clear maximum in Nu for a given Ra and for some $\Omega > 0$. For this investigation we gradually increased ΔT with $\Omega = 0$ until a desired Rayleigh number was reached. After the system came to equilibrium, the Nusselt number was computed from the measured W_F and ΔT . At this point Ω was increased to values between 0 and 300 (corresponding to Taylor numbers between 0 and 4×10^5), and at each value the system was given time to equilibrate. Any adjustments needed in W_F to maintain the same ΔT were made and the resultant Nusselt numbers were then calculated. The uncertainties in W_F and ΔT resulted in a maximum uncertainty in Nu of ± 0.04 . The results of this investigation, as can be seen in figure 7, indicate no maximum Nusselt number for $\Omega > 0$ or for $Pr \approx 0.5$.

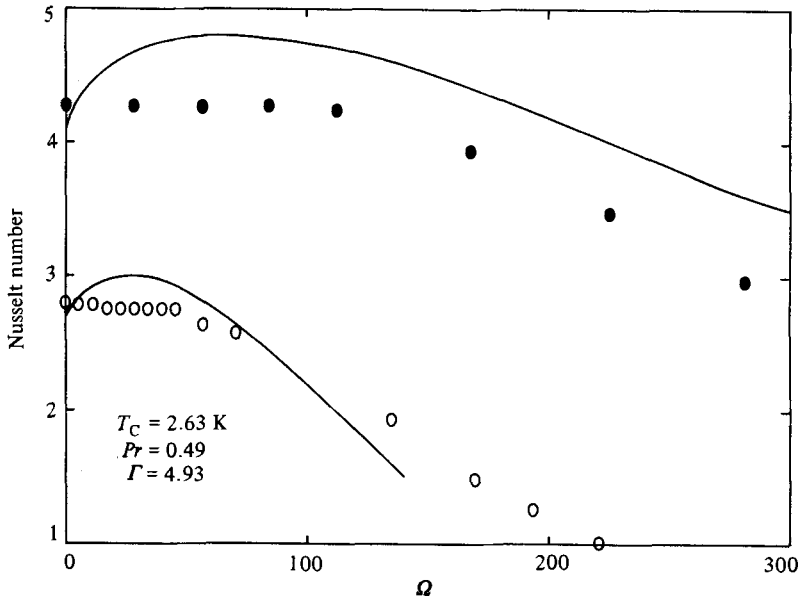


FIGURE 7. Rotational effect on Nusselt number at absolute Rayleigh numbers; Nusselt numbers for fixed Rayleigh numbers as functions of the dimensionless rotation rate Ω : \circ , $Ra = 2 \times 10^4$; \bullet , $Ra = 1 \times 10^5$. The maximum uncertainty of the Nusselt numbers is given by the character size. Solid lines are data given by Rossby (1969) for the same respective Rayleigh numbers but with $Pr = 6.8$.

5. Summary

Some general features expected of the effect of rotation on heat transfer in convection have been verified. In particular, the initial slope characteristic of convective heat transfer increases as Ω is increased from 0. We have also shown that, as expected, the overall effect of rotation is to increasingly inhibit the amplitude of convection motions, and thus the heat transfer, as Ω is increased. There is, however, a range of Pr for which the Nusselt number, measured at $Ra - R_c(\Omega) = 2 \times 10^3$ (or equivalently $d(Nu)/d(Ra)$), displays a maximum for some $\Omega > 0$. This maximum occurs at $\Omega \approx 30$ and in the Prandtl-number range $0.3 < Pr < 0.6$. In contrast to the observations by Rossby of convecting water, normal fluid ${}^4\text{He}$ does not display maximum Nu for a fixed Ra at any Ω other than 0.

Various effects of the finite cell size and shape in convection have been investigated and we have shown that, although the initial slope N_1 increases with Γ at $\Omega = 0$, this behaviour is reversed in the range $100 < \Omega < 250$. Heat-transfer characteristics of the subcritical convection mode have also been investigated and reported here, although we have deferred the detailed discussion of our investigations of characteristics of this convective mode to a future communication.

This research was supported by the National Science Foundation Heat Transfer Program under grant MEA 82-12102. We are grateful to Mr Steve Predko for building the new cells.

REFERENCES

- AHLERS, G., CROSS, M. C., HOHENBERG, P. C. & SAFRAN, S. 1981 The amplitude equation near the convective threshold: application to time-dependent heating experiments. *J. Fluid Mech.* **110**, 297.
- BEHRINGER, R. P. & AHLERS, G. 1982 Heat transport and temporal evolution of fluid flow near the Rayleigh-Bénard instability in cylindrical containers. *J. Fluid Mech.* **125**, 219.

- BEVINGTON, P. R. 1969 *Data Reduction and Error Analysis for the Physical Sciences*. McGraw-Hill.
- CHANDRASEKHAR, S. 1961 *Hydrodynamic and Hydromagnetic Stability*. Clarendon.
- CHARLSON, G. S. & SANI, R. L. 1975 Finite amplitude axisymmetric thermoconvective flows in a bounded cylindrical layer of fluid. *J. Fluid Mech.* **71**, 209.
- CLEVER, R. M. & BUSSE, F. H. 1979 Nonlinear properties of convection rolls in a horizontal layer rotating about a vertical axis. *J. Fluid Mech.* **94**, 609.
- DANIELS, P. G. & STEWARTSON, K. 1977 On the spatial oscillations of a horizontally heated rotating fluid. *Math. Proc. Camb. Phil. Soc.* **81**, 325.
- DANIELS, P. G. & STEWARTSON, K. 1978*a* On the spatial oscillations of a horizontally heated rotating fluid. II. *Q. J. Mech. Appl. Maths* **31**, 113.
- DANIELS, P. G. & STEWARTSON, K. 1978*b* Overstable convection in a horizontally heated rotating fluid. *Math. Proc. Camb. Phil. Soc.* **83**, 329.
- DROPKIN, D. & GLOBE, S. 1959 Effect of spin on natural convection in mercury heated from below. *J. Appl. Phys.* **30**, 84.
- FULTZ, D. & NAKAGAWA, Y. 1955 Experiments on over-stable thermal convection in mercury. *Proc. R. Soc. Lond. A* **231**, 211.
- HOMSY, G. M. & HUDSON, J. L. 1971 Centrifugal convection and its effect on the asymptotic stability of a bounded rotating fluid heated from below. *J. Fluid Mech.* **48**, 605.
- HOMSY, G. H. & HUDSON, J. L. 1972 Stability of a radially bounded rotating fluid heated from below. *Appl. Sci. Res.* **26**, 53.
- HUDSON, J. L., TANG, D. & ABELL, S. 1978 Experiments on centrifugally driven thermal convection in a rotating cylinder. *J. Fluid Mech.* **86**, 147.
- KOSCHMIEDER, E. L. 1967 On convection on a uniformly heated rotating plane. *Beitr. Phys. Atmos.* **40**, 216.
- KÜPPERS, G. 1970 The stability of steady finite amplitude convection in a rotating fluid layer. *Phys. Lett.* **32 A**, 7.
- KÜPPERS, G. & LORTZ, D. 1969 Transition from laminar convection to thermal turbulence in a rotating fluid layer. *J. Fluid Mech.* **35**, 609.
- LUCAS, P. G. J., PFOTENHAUER, J. M. & DONNELLY, R. J. 1983 Stability and heat transfer of rotating cryogenics. Part 1. Influence of rotation on the onset of convection in liquid ⁴He. *J. Fluid Mech.* **129**, 251.
- ROSSBY, H. T. 1969 A study of Bénard convection with and without rotation. *J. Fluid Mech.* **36**, 309.
- SOMMERVILLE, R. C. J. & LIPPS, F. B. 1973 A numerical study in 3 space dimensions of Bénard convection in a rotating fluid. *J. Atmos. Sci.* **30**, 590.
- VERONIS, G. 1958 Cellular convection with finite amplitude in a rotating fluid. *J. Fluid Mech.* **5**, 26.
- VERONIS, G. 1966 Motions at subcritical values of the Rayleigh number in a rotating fluid. *J. Fluid Mech.* **24**, 545.
- VERONIS, G. 1968 Large-amplitude Bénard convection in a rotating fluid. *J. Fluid Mech.* **31**, 113.
- WILLIS, G. E., DEARDORFF, J. W. & SOMMERVILLE, R. C. 1972 Roll-diameter dependence in Rayleigh convection and its effect upon the heat flux. *J. Fluid Mech.* **54**, 351.